Investigation into the Benefits of Reduced Oil Flows in Internal Combustion Engines

R.D. Burke[1], C.J. Brace[1], R Stark[2] and I. Pegg[2]

1. Department of Mechanical Engineering, University of Bath, UK

2. Dunton Technical Centre, Ford Motor Company, UK

Contact author: R. Burke, Department of Mechanical Engineering, University of Bath, Bath, BA2 7AY, UK, +44 (0)1225 383481, R.D.Burke@bath.ac.uk

Abstract

The engine lubrication system is a vital element for engine health but causes a parasitic load on the engine which increases the fuel consumption: this load can be reduced by matching the oil flow to lubricating requirements using a variable displacement oil pump (VDOP). In a first stage, two VDOPs were installed on a 2.4L Diesel engine; experiments over the New European Drive cycle (NEDC) showed reductions in fuel consumption of up to 3.4% and up to 5.8% over the urban phase of the cycle. A VDOP was subsequently installed on an instrumented engine capturing over 100 metal and fluid temperatures within the engine structure. This showed that reducing oil flows resulted in lower oil temperature by up to 4^{o}C during cold start NEDC but

hotter cylinder liner temperatures by up to 6°C. The higher cylinder wall temperatures caused an increase of 3% in NOx emissions but a reduction of 3-5% in CO and Hydrocarbon emissions. Finally an energy flow analysis showed that the VDOP can reduce oil pump energy consumption by 160kJ (32%) but that this led to a 400kJ reduction in friction and accessory work. These findings highlight the need for a systems-level rather than a component-level approach to engine lubrication design to capture key thermal interactions.

Keywords: variable displacement oil pump, thermal management, parasitic losses, systems analysis, Diesel engine, lubrication, Fuel Economy.

1 Introduction

Upcoming legislation for carbon dioxide (CO_2) and fuel consumption will force engine manufacturers to focus on all engine subsystems to exploit even very small benefits [1]. The engine lubricating system is an area where efficiencies can be gained. In most engines lubricant flow is provided by a fixed displacement pump, driven from the crank shaft using a fixed ratio transmission. The primary function is to provide lubricating fluid and cooling to critical parts of the engine, but it is also required to provide hydraulic pressure for lash adjusters, chain tensioners and variable valvetrain systems and the system is designed with each of these aspects in mind. A simplified circuit is shown in figure 1 where the pump speed ω_{pump} is linked to engine speed and the engine characteristics are simplified to a variable orifice which is primarily a function of engine speed. Considering this simplified circuit, the

behaviour of the orifice is described by equation 1. The various components of the oil circuit require a minimum delivery pressure p_{eng}, which for a given engine operating point will be a function only of engine oil flow Q_{eng}. For a particular target p_{eng} at this condition, Q_{eng} is largest when the oil viscosity (ρ_{oil}) is lowest; i.e. when the oil is hottest.

$$Q_{eng} = C_d A_0 \sqrt{\frac{2(p_D - p_{sump})}{\rho_{oil}}} \quad (1)$$

The pump delivery flow Q_T is a function of pump displacement and pump speed and described by equation 2 and for a fixed displacement pump is smallest when the operating speed is lowest. Consequently, the pump displacement D_{pump} must be specified to deliver the minimum pressure p_{eng} with hottest oil and lowest engine speed [2].

$$Q_T = D_{pump}\omega_{pump} \quad (2)$$

At higher pump speeds Q_T increases significantly and to avoid excessively high p_{eng}, a pressure relief valve is installed as shown in figure 1. This will cause a proportion Q_D of the total flow Q_T to flow back to the engine sump. This pressure relief valve needs to be sized for the highest required engine pressure which will typically be at highest engine speed [2]. Consequently at other operating points where pump speed is sufficient to deliver

The hydraulic power delivered by an ideal pump operating in the circuit in figure 1 is given in equation 3. Energy losses will therefore arise whenever Q_T is larger than Q_{eng} or when p_{eng} is

larger than required. In a fixed displacement system sized as described previously, this can arise because of high oil viscosity or mid to high engine speeds where p_{eng} exceeds engine requirements

$$P_{pump} = \frac{Q_T(p_{eng} - p_{sump})}{\eta_{hyd}\eta_{mech}} \quad (3)$$

The use of active systems with a variable displacement pump offer possibilities for avoiding these energy losses by matching oil pump flow Q_T to engine requirements Q_{eng} and avoiding the use of a pressure relief valve [3, 4]. Recent production engines have included such devices to exploit these benefits, however to the authors' knowledge there are no detailed studies of the impacts on engine behaviour [5-8]. The work presented in this paper aims to capture these impacts on the thermal state and quantify the performance benefits in terms of fuel consumption and emissions.

Various reports have been published relating to the use of variable displacement devices with different levels of active control. Rundo and Squarcini [9] only used the device to compensate changes in oil viscosity during engine warm-up. This was achieved by reducing the pump displacement at low oil temperatures where the flow Q_{eng} is lower due to lower (see equation 1). Although experiments were carried out on a dedicated rig rather than on-engine, they predicted a 0.5% reduction in fuel consumption during warm-up. Under warm conditions, the variable displacement device operated as a fixed device but with lower hydraulic efficiency.

Consequently prolonged operation under these conditions resulted in higher power losses compared to the more efficient fixed displacement device (see equation 3) [10].

Various authors [11-13] have highlighted significantly more aggressive approaches to oil flow reduction by varying pump displacement both with oil temperature, speed and load. This approach considers all engine lubricating and cooling requirements, including idling conditions, piston cooling and main bearings, and matches the oil flow over the engine operating range. The use of off-axis variable displacement pump designs also minimized the hydraulic efficiency penalty.

The previous studies have focused on pump driving torque reduction of benefits in fuel economy. However, to the authors' knowledge, the thermal interactions with other engine systems have not been assessed. Because of the inclusion of oil/coolant heat exchangers and piston cooling jets, these interactions could be important. Agarwal and Varghese [14, 15] have assessed the impact of piston cooling jets on piston temperatures. They estimated that piston cooling jets reduce piston temperature by an around 40^{o}C under fully warm conditions. Their work also highlights the impact of jet velocity on piston temperature with a higher velocity reducing piston temperature. In the design of the variable displacement oil pump controller, there will be operating points where piston cooling represents the limiting factor and conditions with a variable displacement device should be very close to those using a conventional fixed displacement device. However, at many operating points the engine

pressure will be lower and this will impact on cooling jet velocity, with subsequent changes in piston temperature.

2 Aims and Objectives

The aim of this work is to characterise experimentally the effects of variable oil flow and its potential benefits for performance both under warm-up and hot engine operating conditions. Reducing the oil flow rate using a variable displacement pump is known to reduce pump work, and therefore reduce engine parasitic losses and improve fuel economy. However this study aims to quantify other system level effects due to changes in the engine cooling and thermal state. Combining these measurements with an in-depth energy analysis will help explain the observed changes in emissions.

3 Experimental Setup

3.1 Engine test setup

3.1.1 Installation and control

Two variable displacement oil pumps (VDOP) and one fixed displacement pump were investigated in this paper. The two variable displacement devices were an internal rotor design (VDOP1) and vane design (VDOP2). Both pumps were installed on a fully run-in 2.4L, 4 cylinder turbocharged Diesel engine. The engine meets euro IV specifications and employed common rail direct injection, variable geometry turbocharger and high pressure, water cooled EGR. The

pumps were sized to have the same maximum displacement as the fixed displacement oil pump which was the engine's production device. As such they could be a direct replacement for the production fixed displacement oil pump and driven directly from the engine crankshaft via a chain drive with similar drive ratio. The engine oil circuit provided oil flows for lubrication and/or cooling of the main bearings, cylinder head and cam shaft bearings, turbocharger and piston crowns through piston cooling jets. An oil to water heat exchanger allowed for cooling of the oil by engine coolant at high operating conditions but equally for heating of the oil when coolant was hotter than oil, for example during warm-up.

The candidate pumps were controlled electro-hydraulically using an algorithm resident within the engine control unit (ECU) which sought to adjust oil pressure as a function of engine speed and load (represented by fuelling demand). The ECU acted open loop, with hydraulic feedback to the pump controlling displacement volume to provide a stable gallery pressure. The pressure set-points maps were adjustable via *Accurate Technologies' (ATi) Vision no-hooks* calibration tool. In this way a standalone passive hydro-mechanical controller was combined with active electronic control to produce a robust yet adaptable system. Clearly a fail-safe design is desirable in a system so critical to engine operation as the oil pump. Mechanically simpler electronic control schemes using direct control of oil pressure do not offer this capability and their operation in the case of a motoring engine and/or electronics failure must be carefully considered.

The engine was installed on a dynamic test stand, loaded by an AC dynamometer. A modified vehicle transmission was used to transmit drive from the engine to the dynamometer shaft, although gear shifts were emulated by the control software rather than enacted in the transmission. The engine was installed as close to in-vehicle setup as possible: the front end auxiliary drive , cooling circuit and air to air intercooler were used in conjunction with a fan emulating road speed external air flows.

Both hot and cold start emulated NEDC experiments were conducted based on the engine being installed in a light commercial vehicle and the appropriate engine speed and brake torque traces for this test are presented in figure 2. The drive cycles were fully automated using CP Engineering Cadet system. For cold start NEDC, the engine was thermally soaked overnight to ensure start temperature of 25^{o}C (+/-1^{o}C). For hot start NEDC, the engine was thermally soaked at 1750rpm/100Nm for 40mins before undertaking the drive cycle ensuring an oil temperature at the start of the NEDC of 95^{o}C (+/-1^{o}C).

3.2 Instrumentation

During the first phase of this work, comparing the fuel consumption benefit of different oil pump designs, fuel consumption was measured both directly using a gravimetric fuel beaker and indirectly based on the carbon balance of engine exhaust gases. These measurements are estimated by equations 4 and 5 respectively. Although high quality measurement devices were used, the installation effects can disturb the measurement systems and affect overall accuracy, therefore techniques previously published by the authors were used to ensure high accuracy

levels, notably for comparing cold and hot start tests [16]. Engine emissions were measured using a Horiba MEXA 7100 analyser system that was calibrated before each experiment to avoid drift issues. The analysers provide a measurement of concentration by volume and the emissions by mass are estimated according to BS ISO standard 8178-1:2006 [17] using equation (6). The specification and accuracy of key measurement sensors is detailed in table 1.

$$M_f = M_{f,b,t_1} - M_{f,b,t_2} \quad (4)$$

$$\dot{m}_{f,CB} = \frac{1}{\frac{w_c}{100}}\left(\frac{w_c}{100}\dot{m}_{HC} + 0.428\dot{m}_{CO} + 0.273\dot{m}_{CO_2}\right) \quad (5)$$

$$\dot{m}_x = K\dot{m}_{ex}c_x\rho_{ratio,x} \quad (6)$$

Type	Location	Sensor	Unit	Accuracy
Air Flow	Engine Air mass flow	ABB Sensyflow	Kg/h	<1% mes.
Emissions	Engine outlet	Horiba MEXA 7100	ppm	1% FS
Fuel flow	Engine fuel consumption	CP Engineering Gravimetric Fuel Beaker	g	+/-0.5% mes or 0.03g
Pressure	Air, Oil	GE PTX Piezoresistive	bar	+/-0.08% FS
Temperature	Metal, coolant	k-type thermocouple	^{o}C	+/-2.2^{o}C
Temperature	Oil	Platinum resistance thermometer	^{o}C	+/-0.3^{o}C

Table 1: Sensor types and measurement accuracy (FS:Full Scale, mes.: Measured Value)

In the second phase of this work, only the vane type variable displacement oil pump was tested on a instrumented engine. A different engine and test facility were used, but of similar type to that in the initial experiments, but clearly some variability would be expected.

Additional instrumentation was installed to measure fluid and engine metal temperatures at over 100 locations in the engine structure. Some sensors were used to measure the temperature at a single point whereas others installed in arrays of three in the cylinder liners to measure temperature gradients between the combustion chamber and the coolant jacket (see figure 3 (a)). These multipoint sensors were arranged at different locations both around and down the bore of cylinders 2 and 3 (see figure 3 (b)). Further thermocouples were installed in each of the five bearing caps to measure both oil film and metal temperatures. The remaining sensors were installed around the internal and external coolant and lubrication circuits.

In cylinder pressure measurements were also recorded to allow an estimate of friction and auxiliary power consumption using the indicator method. These were measured using Kistler 6056A sensors installed in each of the 4 cylinders. Friction and accessory work was calculated as the difference between in indicated and brake works (see equation 7). Indicated work was calculated from in-cylinder pressure measurements (equation 8) whilst brake work was obtained from torque and speed measurements from the dynamometer (equation 9).

$$W_{Fr+Acc} = W_I - W_b \quad (7)$$

$$W_I = \int p_{cy} dV_{cy} \quad (8)$$

$$W_b = \tau_{eng} \times \omega_{eng} \quad (9)$$

This work is aimed at identifying small differences in energy flows as a result of different oil pump control factors. Consequently, the friction and accessory work was corrected for test to test variations in brake work output and alternator work. For the purpose of comparing multiple experiments, each experiment was corrected using the mean alternator and brake works according to equation 10; this removes significant experimental noise factors and allows for better comparison of measured results.

$$W_{Fr+Acc,CORR,i} = W_{Fr+Acc} - \left(W_{alt,i} - W_{alt,mean}\right) - \left(W_{b,i} - W_{b,mean}\right) \quad (10)$$

The alternator work was estimated using measured voltage and current and estimated mean alternator efficiency using equation 11.

$$W_{alt} = \eta_{alt} \times v_{alt} \times I_{alt} \quad (11)$$

3.3 Flow test setup

The fixed displacement and variable displacement vane pumps (VDOP1) were installed on a dedicated flow rig. This facility uses an electric motor to drive the oil pump which pumps oil against a calibrated orifice emulating the engine. The orifice diameter was adjusted for different oil temperatures to match pump back-pressure to that observed on engine for an engine speed of 2000rpm. This installation allows direct measurement of oil flows and oil pump torque. Oil pump speed sweeps were conducted for a range of target oil pressures and

at a range of equivalent oil temperatures. For low temperatures, actual engine oil was used however for operating points above the upper temperature limit of the flow rig, an alternative oil was used with a viscosity at low temperature equivalent to that of engine oil at high temperature. It should be noted that whilst this matches the fluid viscosity, pump operating temperatures are considerably lower which would affect thermal expansion of the device and notably any leakage flows which could cause discrepancies with the behaviour observed on-engine.

The results from the flow test were subsequently used to define the non-linear relationship between oil pump speed, supply pressure and engine torque (equation 12). By using the measured engine speed N_{eng} and the gear ratio between crank and oil pump $R_{oilpump}$, the oil pump power can be estimated throughout the NEDC (equation 13). Integrating this power over the cycle results in the energy consumption from the oil pump (equation 14).

$$\tau_{oil\ pump} = f\left(N_{eng}, p_{oil}, T_{oil}\right) \tag{12}$$

$$P_{oil\ pump} = \tau_{oil\ pump} \times \frac{2\pi N_{eng}}{60} \times R_{oilpump} \tag{13}$$

$$W_{oilpump} = \int P_{oilpump} \tag{14}$$

3.4 Repeatability and Uncertainty Analysis

In the context of the engine system, the oil circuit represent only a small proportion of the energy consumption and therefore errors in the measurement process can be of the same order as the expected results. In this study, two types of errors are considered:

1. Systematic errors through the uncertainty of the measurement system due to the accuracy of the measurement sensors.
2. Random errors due to factors beyond the control of the test facility which result in variation between repeated experiments for the same operating condition.

3.4.1 Systematic errors

Systematic errors result from inaccuracies in the measurements system and offsets in the setting of the operating points on the engine. In this work only those associated with the measurement system are considered. The uncertainty associated with each of the sensors is linked to the accuracy of these sensors as described in table 1. When these measurements are combined to estimate emissions, fuel consumption and energy flows (equations 5-7 and 9-13) these errors can propagate and amplify [18]. Each estimated quantity *y* is calculated based on a number of inputs x_i (equation 15). The uncertainty of each quantity *y* is u_y and is calculated using equation 16.

$$y = f(x_1, x_2, \dots, x_i, \dots, x_n) \qquad (15)$$

$$u_y = \sqrt{\sum_{i=1}^{n} \left(\frac{\partial y}{\partial x_i} u_{x_i} \right)^2} \qquad (16)$$

Emissions and total work are estimated over the complete NEDC drive cycle as the sum of 1180 instantaneous measurements, recorded on a 1Hz basis over the drive cycle (equation 17, with Δt=1 for 1Hz data acquisition).

$$Y = \sum_{t=1}^{1180} x_t \, \Delta t \qquad (17)$$

In this case, the combined value *Y* for the whole drive cycle is a result of a large number of individual measurements x_t at each time point *t*. Because the same instruments are used for each x_t, the measurements are correlated and the combined uncertainty of *Y*, u_Y must be calculated using equation 18 in place of equation 16.

$$u_Y = \sum_{t=0}^{1180} u_{x_t} \, \Delta t \qquad (18)$$

Total fuel consumption measured using the gravimetric fuel beaker is a third case where the drive cycle fuel consumption is estimated by the difference of fuel weight between the two instances of time (equation 4). In this case, the uncertainty is given by equation 19.

$$u_{M_f} = u_{M_{f,b,t=0}} - u_{M_{f,b,t=T}} \quad (19)$$

3.4.2 Random errors

To capture the effects due to random errors, each test condition was repeated at least six times and each of these experiments was analysed to identify any anomalous behaviour both of the engine and test bed. For each test condition, these repeat tests were used to calculate 95% confidence intervals using equation 20. The nominator of this equation is the standard deviation of the measurements and directly affected by the random test-to-test variation. Increasing the number of tests reduces the confidence interval both directly through the denominator and by changing the t value for a given confidence interval. Tighter confidence intervals allow for the demonstration of smaller differences between different test conditions, in this case different oil flows, if it is assumed that the systematic errors are the same in both cases.

$$CI_{95\%} = \frac{\sqrt{\frac{\sum_{i=1}^{n}(y_i - \bar{y})^2}{n-1}}}{\sqrt{n}} t_{n,95\%} \quad (20)$$

Where n is the total number of measurements y_1, y_2, y_i…y_n; $\bar{y}$ is the mean of the measurements and $t_{n,95\%}$ is the two-tailed probability from student's t-distribution for n measurements and 95% confidence interval.

4 Results

4.1 Oil Pump Control

During the first phase of the work, the target oil pressure was set to a constant 3bar gauge for both variable displacement oil pumps, although at lower engine speeds this was not always achievable. This level was chosen arbitrarily as a mid-point between the fixed displacement pump delivery pressure and the minimum allowable engine delivery pressure. Two sets of tests were performed to assess the transient pressure control performance of the two variable displacement pumps. Both tests consisted of an engine speed sweep with the engine hot and oil temperature at 90^{o}C. In the first test, the speed was increased from 800 to 4000rpm in 300seconds and subsequently reduced at the same rate, thus representing quasi-steady state behaviour. In the second test, the speed was swept from 800 to 4500rpm in 5seconds to capture transient performance.

The slow transient test results are shown in Figure 4 (a). These show that the Vane pump stabilises at the 3bar target pressure at a lower engine speed than the internal rotor pump. Subsequently, the vane pump adheres to the target more accurately than the internal rotor design.

The results for the slow response test are shown in Figure 4 (b). This shows that again the vane pump stabilised at the 3bar target pressure at a lower engine speed and is subsequently more

accurate at maintaining the constant pressure. Both pumps show evidence of hysteresis loops, however the vane pump performed significantly better in this regard.

The controlled oil pressures over a cold start NEDC are shown in Figure 5 for the fixed displacement and both variable displacement pumps. The high oil pressures generated with the fixed displacement device when the oil is cold are not apparent with either VDOP, although the internal rotor pump does overshoot the target pressure over the first 100seconds. As the oil warmed up, the pressure delivery from both VDOP dropped below the target 3bar despite the controller ensuring they were delivering full flow output. Both pumps were sized to deliver suitable flow rates at hot idle conditions. The vane-type pump had worse efficiency at these conditions compared to the internal rotor design and therefore necessitated a higher nominal flow volume. At the modest temperature seen during the cold start drive cycle, this resulted in higher flow rates and delivery pressure. An undesirable consequence of this would be an increase in driving torque relative to the other pumps under this operating condition.

For the second phase of the work, using only the internal rotor pump, three different strategies were used. To simplify notation in the results section, these will be referred to as build 1 to 3 as defined by table 2.

Build	Oil Pump	Target oil pressure
1	Fixed Displacement	N/A
2	Vane VDOP	3bar (flat map)
3	Vane VDOP	1-2bar (optimized)

Table 2: Build numbers for experimental campaign

These three different calibrations are illustrated in the form of engine supply pressure against engine speed and oil temperature in figure 6. Also shown is the behaviour of the fixed displacement pump. This demonstrated excellent control of the oil pressure for both the flat map and optimized setups. In the flat map calibration, the pump is not able to meet the pressure demand with maximum displacement volume at high oil pressures and low engine speed because of the lower oil viscosity under these conditions.

Although the engine supply is of primary interest in terms of engine health, the oil flows through an external circuit comprising of the filter and oil/coolant heat exchanger before arriving in the ladder frame. This external circuit represents a pressure loss and to understand the pump behaviour it is also interesting to assess the pump delivery pressure. This is shown in the same format as above in figure 7.

These show that the VDOP has similar behaviour to the fixed displacement pump when used under max flow calibration. Under these conditions, both pumps deliver oil pressures above 6bar when cold, gradually reducing to around 4bar when the oil is hot. In the reduced flow configurations, the opposite is true as the pump needs to supply a larger flow to meet the pressure set-point in the main gallery. Consequently, there is a larger pressure loss in the external circuit, and the pump supplies a larger pressure under fully warm conditions.

4.2 Phase 1: Comparison of different VDOPs

Each of the fuel consumption estimates gave similar trends in results and only the gravimetric measurements are presented in this work. These are presented for cold start and hot start

NEDC tests in table 3 and table 4 respectively. In each case the number of tests is given along with the 95% confidence intervals for each measurement set. For all conditions this was below +/-0.5% and significantly smaller than the absolute differences in fuel consumption between pumps.

For cold start NEDC the Internal rotor pump offered 3.4% reduction in fuel consumption over the NEDC whilst the vane pump offered 2.6%. The proportion of fuel consumption benefit is larger for the urban phase (ECE) when the oil was coldest and more viscous. This phase also corresponds to lower engine power output so the impact of improvements to parasitic losses would be expected to be more significant. Finally although vehicle speeds are much higher during the extra urban phase, engine speeds and therefore pump speeds are actually higher during the ECE, as shown in figure 2. For the hot start NEDC, the internal rotor pump offered 2.3% improvement and fuel consumption and the vane pump 1.7%. Again, there was a more noticeable benefit during the urban phase.

Pump	NEDC Phase	No. of Tests	Mean FC (g)	Standard Error 95% confidence interval		FC improvement vs. Fixed Disp. (%)
				(+/- g)	(+/-%)	
Fixed Disp.	ECE	7	374.3	2.0	0.5%	-
	EUDC		486.1	0.9	0.2%	-
	NEDC		860.5	2.7	0.3%	-
Internal rotor	ECE	7	352.6	1.6	0.4%	5.8%
	EUDC		478.6	1.0	0.2%	1.6%
	NEDC		831.1	1.5	0.2%	**3.4%**
Vane	ECE	8	359.2	0.7	0.2%	4.1%
	EUDC		478.8	0.8	0.2%	1.5%
	NEDC		838.0	0.9	0.1%	**2.6%**

Table 3: Cold start NEDC fuel consumption performance for fixed and variable displacement oil pumps

Pump	NEDC Phase	No. of Tests	Mean FC (g)	Standard Error 95% confidence interval		FC improvement vs. Fixed Disp. (%)
				(+/- g)	(+/-%)	
Fixed Disp.	ECE	12	339.2	1.1	0.3%	-
	EUDC		491.2	0.4	0.1%	-
	NEDC		830.4	1.3	0.2%	-
Internal rotor	ECE	13	327.5	1.2	0.4%	3.5%
	EUDC		483.8	0.6	0.1%	1.5%
	NEDC		811.3	1.2	0.2%	**2.3%**
Vane	ECE	16	331.4	1.2	0.4%	2.3%
	EUDC		484.6	0.7	0.1%	1.3%
	NEDC		816.0	1.4	0.2%	**1.7%**

Table 4: Hot start NEDC fuel consumption performance for fixed and variable displacement oil pumps

4.3 Phase 2: Thermal analysis of Vane pump

4.3.1 Fuel Consumption and Emissions

Fuel consumption measurements for all tests are presented in figure 8 with 95% confidence intervals for each phase of the NEDC cycle and for cold- and hot-start tests. These results show good repeatability allowing statistically significant differences between test configurations to be demonstrated. The fuel consumption results presented are from the gravimetric fuel balance, however this agreed well with the carbon balance method.

Similar benefits in fuel consumption were observed as in phase 1, with further benefits obtained by reducing the target oil pressure below the 3 bar level. The optimized oil pressure set-point (*build 3*) offered a 36g (4%) benefit over the fixed displacement pump for cold start tests. This can be split into 22g (6%) during phase 1 and 14g (3%) over phase 2.

Oxides of nitrogen (NOx), hydrocarbon (HC) and carbon monoxide (CO) emissions, sampled between the turbocharger and the catalyst, for phases 1 and 2 are shown for cold- and hot-

start tests in figures 9 and 10 respectively. The spread of data is larger than fuel consumption showing poorer repeatability for these measurements, however significant trends are still apparent. In most conditions, NOx emissions are up to 3% higher with reduced oil flow. The exception to this is phase 1 of the cold-start drive cycle where NOx emissions are 5% lower. HC and CO emissions follow similar trends throughout and tend to reduce by 3% to 5% with lower oil flow. Phase 1 of the cold-start drive cycle shows the smallest effect with larger effects during hotter engine running.

Uncertainties associated with systematic errors in the instrumentation for fuel consumption and emissions are summarised in table 5. For fuel consumption, the uncertainty is very low (0.05%) because the estimate is a result of the difference of two measurements using the same instrument. In this case, the uncertainty of one measurement is almost completely cancelled out by that of the second measurement. In contrast for emissions, the uncertainties are all in the region of 7-13% for Urban cycle, but can be lower in the extra urban cycle. This is a result of the similar relative accuracies of the emissions analysers (table 1), and the use of a common exhaust mass flow measurement. The higher accuracy during the extra urban phase is a result of the lower relative uncertainty of the mass flow measurement.

	Cold Start			Hot Start		
	UDC	EUDC	NEDC	UDC	EUDC	NEDC
FC	0.18g *(0.05%)*	0.26g *(0.05%)*	0.44g *(0.05%)*	0.17g *(0.05%)*	0.26g *(0.05%)*	0.43g *(0.05%)*
NOx	0.16g *(13%)*	0.29g *(7.5%)*	0.45g *(9%)*	0.17g *(12%)*	0.33g *(8%)*	0.5g *(9%)*
CO	1.8g *(9%)*	0.25g *(3.5%)*	2.05g (8.2%)	0.8g (10%)	0.15g *(2.7%)*	1.05g *(7.8%)*
HC	0.23g *(8.2%)*	0.02g *(3%)*	0.25g *(6.9%)*	0.15g *(8.8%)*	0.05g *(6.3%)*	0.2g *(8%)*

Table 5: Instrumentation based uncertainty for fuel consumption and emissions measurements (UDC: Urban phase of NEDC, EUDC: Extra-urban phase of NEDC)

4.3.2 Thermal behaviour

In this section a number of time series plots will be presented showing the evolution of various temperatures during the NEDC tests. In each case, the lines presented represent the average behaviour for all repeat tests; this avoids analysing extreme differences between any two particular tests.

Figure 11 (a) shows main gallery oil temperature for different oil pumping pressures and for both hot- and cold-start tests. It is clear from the cold-start tests that a reduced oil flow leads to reduced oil temperatures in the main gallery by up to 4^{o}C during warm-up. This may be explained by reduced work input to the lubricant and less heat generation in the pressure relief valve, but also because of less overall heat transfer to the oil around the engine, notably in the piston and bore regions because of reduced flow. During the hot start tests there is less than 1^{o}C difference between the different flow strategies. This has a knock on effect for the temperature of key lubricating surfaces such as the crank shaft bearings (figure 11 b) and valve train bearing caps (figure 11 c). During warm-up, the crank and valve train bearing caps are 1-3^{o}C colder with reduced oil flow: this is accounted for by less heat being delivered to these

regions of the engine in the colder lubricant. Under hot conditions, the differences are less than 1°C. It should also be noted that under hot conditions, the crank bearing caps were hotter with lower oil flow rates.

A selection of liner temperatures showing key differences over the first 600 seconds of the cold-start NEDC are shown in figure 12. These include temperatures down the bore, at different depths and on intake and exhaust sides. A small diagram is also shown indicating thermocouple locations. From these temperature profiles, it is clear that the reduction of oil flow does have an effect on cylinder liner temperatures. These are most marked in the lower half of the stroke, closer to the combustion chamber (figure 12 b, d and e). After 200 seconds, lower liner temperatures in the test with lowest oil flow lead the fixed displacement setup by 4-6°C. Temperatures at the top of the cylinder are much less affected by the oil flow (figure 12 a); in this position after 200 seconds the lowest oil flow setup leads the fixed displacement oil pump by only 2°C. Deeper into the liner, away from the combustion chamber temperatures are also less affected by oil flow rate (figure 12 c) with a difference of less than 1°C between setups. Temperatures nearer bottom of the liner and further away from the coolant jacket would be expected to be more dependent on oil cooling effects. The variations in liner temperatures here are of similar order or magnitude to the simulated piston temperature changes reported by Agarwal and Varghese [14, 15].

In addition to differences down the cylinder bore, there are also differences comparing exhaust and intake sides of the engine (figure 12 d and e). On the intake side, after 200

seconds the low flow test leads the fixed displacement build by 4°C, whereas on the exhaust side at this same time the difference is 6°C. In all tests, after 600 seconds the temperatures on intake side appear to be converging as the engine warms up, however on the exhaust side the higher temperature prevails longer. These differences may be a result the different piston forces acting on the liner on the thrust and anti-thrust sides.

Figure 13 shows the same temperature measurement as figure 12 (d), but for both hot and cold-start tests and for the whole NEDC. Despite a convergence of liner temperature at around 800 seconds in the cold-start tests, under fully warm conditions, the experiments with lower oil flow operate 2-6°C hotter than with the fixed displacement pump. This convergence of temperatures is explained by interaction with the coolant temperature during warm-up. Because the oil is slightly cooler with the low oil flow configurations, this reduces the coolant temperature relative to the production pump. This colder coolant causes slightly colder liner temperatures which cools the liner temperature to a similar level of that using the fixed displacement pump. Although these temperatures are the same, they are achieved through different levels of coolant and oil cooling.

4.4 Oil pump and friction power

Indicated results were recorded on subsequent cold start experiments with the three VDOP calibrations (max flow, flat map and optimised). Figure 14 shows friction and accessory power and cumulative work over the NEDC cycle. The uncertainties associated with these estimated are summarised in table 6. The power plot is difficult to assess due to significant noise present

during the transient phases (mainly a result of difficulties in aligning indicated and brake measurements). Integrating this signal to estimate work allows easier assessment of the results. The differences resulting from variations in oil flow are small in the context of overall friction and accessory loading; however there is a trend of reduced work with reduced oil flow.

To quantify the oil pump work, separate tests were conducted on a dedicated flow rig and the measured oil flows and driving torques for the fixed and variable displacement pumps are shown in figures 15 and 16 respectively. The test bench results clearly showed a reduction in oil flow from the VDOP compared to the fixed displacement pump. There are also changes in flow rates as a result of the change in temperature (or viscosity) of the oil. At 110^{o}C the flow was 10L/min higher for the baseline pump compared the 60^{o}C condition. The VDOP delivers approximately 7-11L/min (20-40%) lower flow with a 3bar target pressure and 10-15L/min (40-50%) with 2bar target at 60^{o}C. With oil at 110^{o}C similar reductions were measured. The reduction in pump driving torque for the VDOP compared to the baseline pump was similar at 60^{o}C and 110^{o}C and was between 1-3Nm (40-75%) over the speed range. These observed reductions are the result of both the reduced displacement and the reduced delivery pressure.

The measurements from the flow rig can be used to estimate the required torque to drive the oil pump, the power consumption and the total energy consumed over the NEDC tests. Figure 17(a) shows the energy consumption of the oil pump for builds 1 and 3 relative to the total friction and accessory energy calculated previously from indicated and brake work. The uncertainty estimates are given in table 6. It can be seen that the oil pump work accounts for

approximately 6-8% of total work. It is estimated that oil pump energy consumption reduces from 500kJ in the max flow condition to 340kJ in the optimised build 3 conditions. This is lower than the measured difference in total friction and accessory load which reduced from 5,800kJ to 5,400kJ. These differences are larger than the uncertainty associated with these measurements.

	Inst. Average (%)	Urban (kJ)	NEDC (kJ)
Fr + Acc	5.3%	150 (4.3%)	280 (5.3%)
Oil Pump	4.1%	10 (4%)	17 (4.1%)

Table 6: Uncertainty estimates for Friction/Accessory work and Oil Pump work

Figure 17(b) shows the corrected friction and accessory work over the NEDC against the oil pump work and the 95% uncertainty margins in both axes. Also shown is a hypothetical $\Delta y=\Delta x$ line; this represents the line on which all data points would lie if the variation in oil pump work were equal to the observed reduction in friction and accessory work. As can be seen, the measurements of friction and accessory work all lie below this line which means that these changes exceed the reductions in oil pump work alone: for a reduction in oil pump work of 160kJ, the friction and accessory work reduced by 400kJ, approximately 2.5 time larger. This may be explained by the system effects of the reduced oil flow which have been seen to affect key temperatures of the friction surfaces during warm-up.

5 Discussion

The introduction of a variable displacement oil pump offers an additional control parameter for the engine. Initial results demonstrated a clear benefit in fuel consumption from the lower

oil flow rates. Subsequent in-depth analysis of the engine operating behaviour has demonstrated that there are some direct effects of reducing the oil flow which include lower oil pump work. Some secondary effects on oil, coolant and metal temperatures were also measured. Each of these will have different effects on fuel consumption and emissions. Fuel consumption benefits were consistent between the two separate experimental campaigns of this work, offering up to 4% improvement in fuel consumption over the cold start NEDC. Higher benefits were observed during the ECE urban phase; this difference is attributable to a number of factors: firstly the engine brake loads are lower in the first phase meaning friction and parasitic losses are proportionally more significant to overall fuel consumption. Secondly, although vehicle speeds are lower during this phase compared to the EUDC, the engine speeds are higher meaning the oil pump speed will also be higher: results from the flow rig showed that the benefits of VDOP were more important at higher pump speed.

Liner temperatures were highest in all tests with lowest oil flow. Under hot conditions, these tests also produced the highest NOx emissions and lowest HC and CO emissions (Hot tests and phase 2 cold tests). When the engine is operating fully warm there are no discrepancies in the injection timing meaning the differences in emissions can be largely attributed to the differences in temperatures. However, during warm-up NOx are reduced with low oil flow and there is little effect on HC and CO emissions. This trend is not obvious because the higher liner temperatures would suggest an increase in combustion temperatures and therefore NOx emissions as under all other measured conditions. Nevertheless, there are two possible

explanations for this phenomenon: The first is that the reduction in fuel consumption through reduced oil flow reduces the quantity of fuel burnt in the cylinder which in turn would increase the air to fuel ratio and therefore reduce combustion temperatures. The second possible explanation notices that the oil is colder with lower oil flow during warm-up unlike during fully warm operation. As the oil provides cooling to the pistons, depending on the thermal contact with the cylinder liner, this may reduce the piston crown temperature and also combustion gases. A more detailed investigation of cylinder cooling is required to investigate these hypotheses.

The effects of the VDOP offer a trade-off between fuel consumption and NOx emissions in a similar way to injection timing and EGR. However, unlike these other control mechanisms, this approach is very favourable to fuel consumption and should offer significant benefits. The installation of such a device should be done in conjunction with a re-calibration of the control strategy to ensure emissions regulations are met.

The reduction in engine friction and accessory load was seen to be greater than the reduction in oil pump driving torque alone. It should be noted that measurement uncertainties associated with the results are large due to its reliance on the ill conditioned indicator method and the estimate of oil pump work from off-engine measurements. Nevertheless, the results highlight the requirements for a systems based approach rather than a component level approach when conducting research into oil pump work as the influence on engine behaviour is significant both from and friction and emissions formation perspective. This work also

highlights the need for more detailed friction measurements in the firing engine to isolate where additional benefits are achieved.

This study has been performed on a recent Diesel engine, however as more requirements are added to the lubrication circuit with future IC engine developments, the benefits from a variable displacement device may become even larger.

6 Conclusion

An on-engine experimental investigation into the macroscopic and thermal effects of a variable displacement oil pump has been conducted.

1. Active control of the oil flow using a variable displacement pump avoids excessive energy loss in a pressure relief valve and significantly reduces the pump driving torque, measured as a reduction in indicated work. This can provide a fuel consumption saving of 4% over cold- and hot-start NEDCs. These benefits would be expected to be larger in a duty cycle with more extensive high engine speeds.
2. Varying oil flow has a significant effect on the thermal state of the engine: cylinder liner temperatures were up to 6^{o}C hotter with reduced oil flow rates. Measurements showed that lower liner temperatures were more strongly affected. In contrast, oil temperatures were 4^{o}C lower during warm-up but 1^{o}C hotter under fully-warm conditions.

3. The changes in thermal state had a knock-on effect on engine emissions: with lower oil flow NOx emissions increased by 3% except during warm up where they reduced by 1.5%. The reduction is not consistent with the measured variations in liner temperatures and requires a more detailed investigation into cylinder cooling. HC and CO emissions were always reduced by 3-5% with low oil flow.
4. The calibration of the variable displacement oil pump creates a trade-off between fuel economy and NOx emissions which should be included in engine calibration procedures. However unlike most control mechanisms such as EGR and injection timing, this approach is very favourable to fuel economy, giving scope for significant benefits.
5. Within the accuracy of the correlations between rig and engine testing, the reduction in friction and accessory load appears to be 2.5 times larger than the reduction in oil pump driving torque, owing to system effects within the engine. This highlights the need for a system level rather than a component level approach to the development of engine lubricating systems.

Acknowledgements

Selected sections and figures contained within this work have been reproduced with permission from ASME, originally presented at the ASME Internal Combustion Engine Spring Conference, Turin, Italy, May 2012.

Funding

The authors would like to acknowledge the funding from the Technology Strategy Board [TSB project No: TP/9/LCV/6/I/S0052K].

Appendix

Abbreviations

CO	Carbon monoxide
ECE	Urban phase of NEDC
ECU	Engine Control Unit
EGR	Exhaust Gas Recirculation
EUDC	Extra Urban phase of NEDC
FC	Fuel Consumption
HC	Hydrocarbons
NEDC	New European Drive Cycle
NOx	Oxides of Nitrogen
VDOP	Variable displacement Oil Pump

Notation

A_o	Orifice Area	m^2
$CI_{95\%}$	95% confidence interval	-
c	emission concentration	ppm or %
C_d	Orifice discharger coefficient	
D	Pump displacement volume	m^3
I	current	A
K	Dry/Wet emission correction factor	
m	mass	kg
$\dot{m}$	mass flow	kg/s
n	number of repeat tests	-
N	Rotational Speed	rev/min
p	Pressure	Pa/bar
P	Power	W
Q	Volumetric flow	m^3/s
R	Gear Ratio	
T	Temperature	K
t	time	s
$t_{n,95\%}$	student's t value for n tests at 95%	-
u	uncertainty	
V	voltage	V
w_c	Fuel carbon content by mass	%

W	Work	J
x	independent variable	
Y	Cumulative Measured Variable	
y	Measured Variable	-
$\bar{y}$	Mean measured variable	-
ρ_{oil}	Oil Density	kg/m^3
ρ_{ratio}	Emissions Relative Density factor	
η	Efficiency	
τ	Torque	Nm
ω	Rotational speed	rad/s

Subscripts

alt	Alternator
b	Brake
CB	Carbon Balance
CO	Carbon Monoxide emissions
CO_2	Carbon Dioxide emissions
CORR	Corrected
D	Dump
cy	Cylinder
eng	Engine
Fr+Acc	Friction and Accessory
f	fuel
g	Gravimetric Beaker
HC	Hydrocarbon Emissions
I	Indicated
i	numeration
oil	Oil main gallery conditions
oilpump	Oil pump
s	Swept
T	Total
t	time
x	emission species

References

[1] N. Owen and N. Jackson, A new look at the low carbon Roadmap, presented at the Low-Carbon Vehicles 2009, London (UK), 2009.

[2] Q. Zhou, Engine Lubrication System Analysis and Oil Pump Design Optimization. In: Luo J., Meng Y., Shao T., Zhao Q., (eds.). Advanced Tribology: Springer Berlin Heidelberg, 2010, p. 56-60, DOI: 10.1007/978-3-642-03653-8_23, ISBN: 978-3-642-03652-1

[3] S. Loganathan, S. Govindarajan, J. Suresh Kumar, K. Vijayakumar, and K. Srinivasan, Design and Development of Vane Type Variable flow Oil Pump for Automotive Application, SAE Paper 2011-28-0102.

[4] J. Meira, A. Filho, W. Melo, and E. Ribeiro, Strategies for Energy Savings with Use of Constant and Variable Oil Pump Systems, SAE Paper 2011-36-0150.

[5] P. Werner, J. Schommers, U. Engel, C. Spengel, C. Reckzugel, M. Paule, T. Maderstein, and W. Eisler, The New V6-Diesel Engine from Mercedes-Benz, presented at the 19. Aachener Kolloquium Fahrzeug- und Motortechnik 2010, Aachen, Germany, 2010.

[6] F. Steinparzer, H. Unger, T. Bruner, and D. Kannenberg, The new BMW 2.0 litre 4-cylinder S.I. engine with twin Power Turbo Technology, presented at the 32. Internationales Wiener Motorsymposium, Vienna, 2011.

[7] T. Heiduk, R. Dornhofer, A. Eiser, M. Grigo, A. Pelzer, and R. Wurms, The new generation of the R4 TFSI engine from Audi, presented at the 32. Internationales Wiener Motorsymposium, Vienna, 2011.

[8] E. Blanchard, J. Visconti, P. Coblence, F. Legrand, F. Gautier, M. Chevrot, M. Clautet, and F. Trochu, The New Renault dCi 130 1.6l Diesel engine, presented at the 19. Aachener Kolloquium Fahrzeug- und Motortechnik 2010, Aachen, Germany, 2010.

[9] M. Rundo and R. Squarcini, Experimental Procedure for Measuring the Energy Consumption of IC Engine Lubricating Pumps during a NEDC Driving Cycle, SAE paper number 2009-01-1919.

[10] D. Staley, B. Pryor, and K. Gilgenback, Adaptation of a Variable Displacement Vane Pump to Engine Lube Oil Applications, SAE paper number 2007-01-1567.

[11] F. Toyoda, Y. Kobayashi, Y. Miura, and Y. Koga, Development of Variable Discharge OilPump, SAE paper number 2008-01-0087.

[12] P. G. Evans and K. Johanson, The System Performance Benefits of Lubrication Flow Control, SAE paper number 2004-01-2687.

[13] H. Neukirchner, M. Kramer, and T. Ohnesorge, The controlled vane-type oilpump for oil supply on demand for passenger car engines, SAE paper number 2002-01-1319.

[14] A. K. Agarwal and M. B. Varghese, Numerical investigations of piston cooling using oil jet in heavy duty diesel engines, *International Journal of Engine Research,* vol. 7, pp. 411-421, 2006.

[15] M. B. Varghese, S. K. Goyal, and A. K. Agarwal, Numerical and Experimental Investigation of Oil-Jet-Cooler Piston, SAE paper number 2005-01-1382.

[16] R. D. Burke, C. J. Brace, and J. G. Hawley, Critical analysis of on-engine fuel consumption measurement, *Proceedings of the Institution of Mechanical Engineers Part D-Journal of Automobile Engineering,* vol. 255, pp. 829-844, 2011.

[17] BS ISO 8178-1:2006, Reciprocating internal combustion engines. Exhaust emission measurement. Test-bed measurement of gaseous and particulate exhaust emissions, Second Edition, 2006.

[18] Anon, *Guide to the expression of uncertainty in measurement (GUM), JCGM 100:2008(E),2008,* Available: http://www.iso.org/sites/JCGM/GUMJCGM100/C045315e-html/C045315e.html?csnumber=50461 (accessed 30/07/2009)

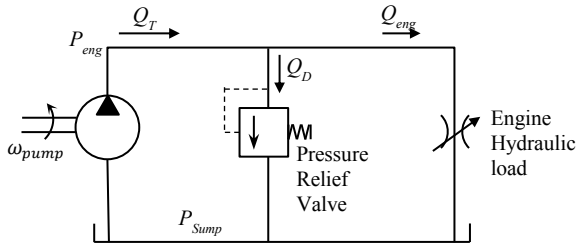

Figure 1: Simplified hydraulic circuit of engine lubricating system to illustrate pump loading

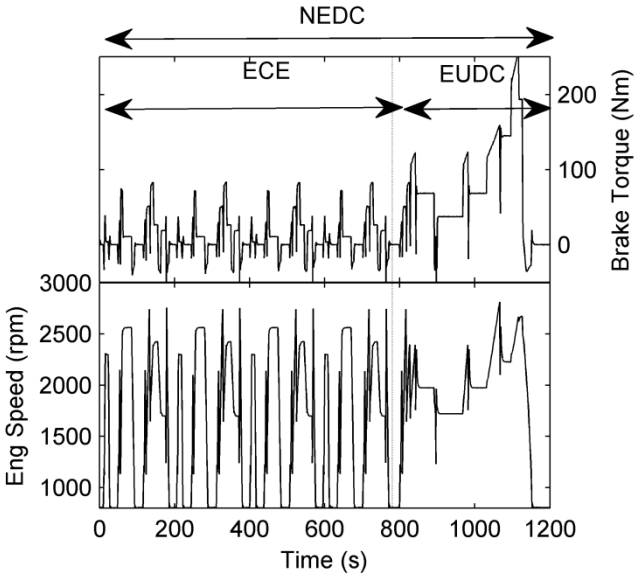

Figure 2: NEDC engine speed and torque traces showing split between urban (ECE) and extra-urban (EUDC) phases

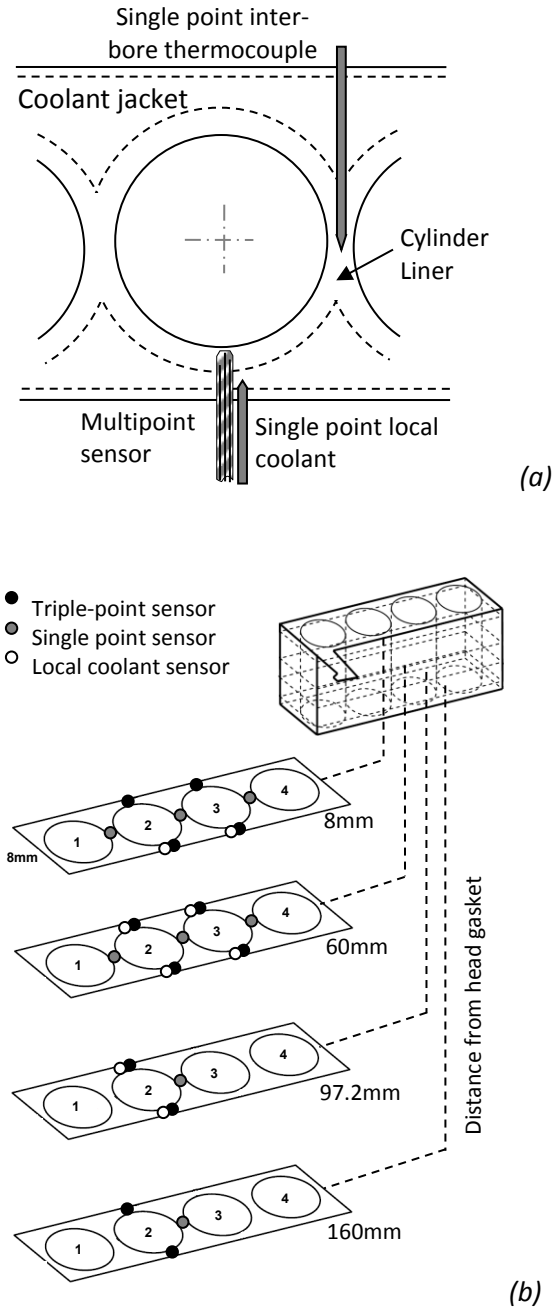

Figure 3: (a) Detailed view of thermocouple layout around the cylinder liners and (b) overall view of thermocouple positions in the engine block

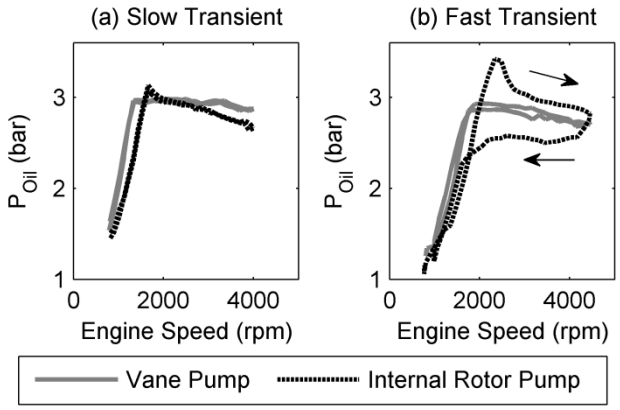

Figure 4: Variable displacement oil pump pressure response control for (a) fast transient and (b) slow transient

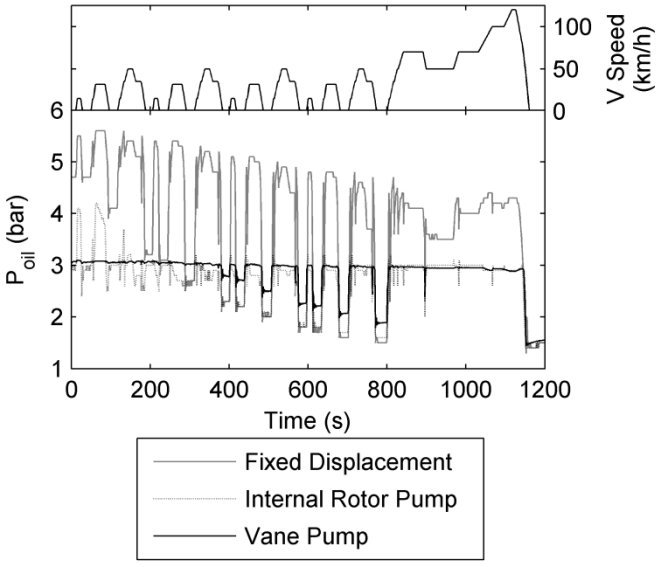

Figure 5: Delivery pressure over NEDC cycle for fixed displacement and both variable displacement oil pumps with target delivery pressure of 3bar

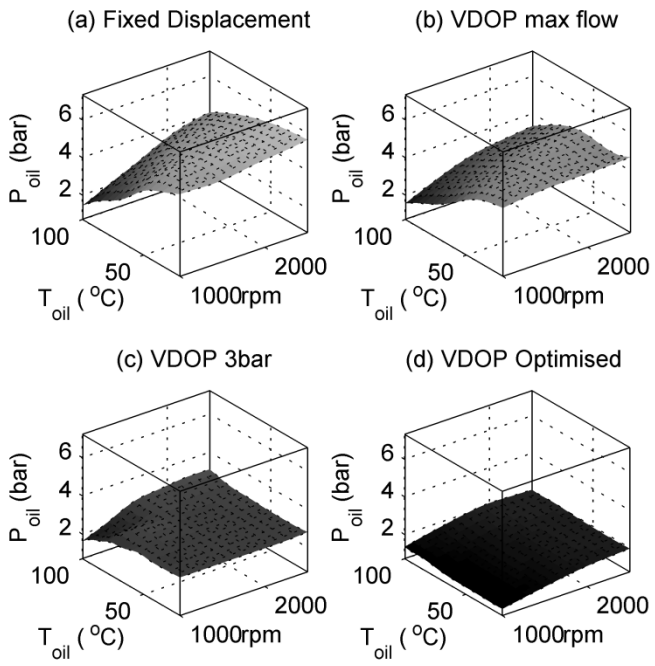

Figure 6: Engine supply oil pressure against engine speed and oil temperature for (a) fixed displacement oil pump, (b) max flow VDOP, (c) flat map VDOP and (d) optimized VDOP

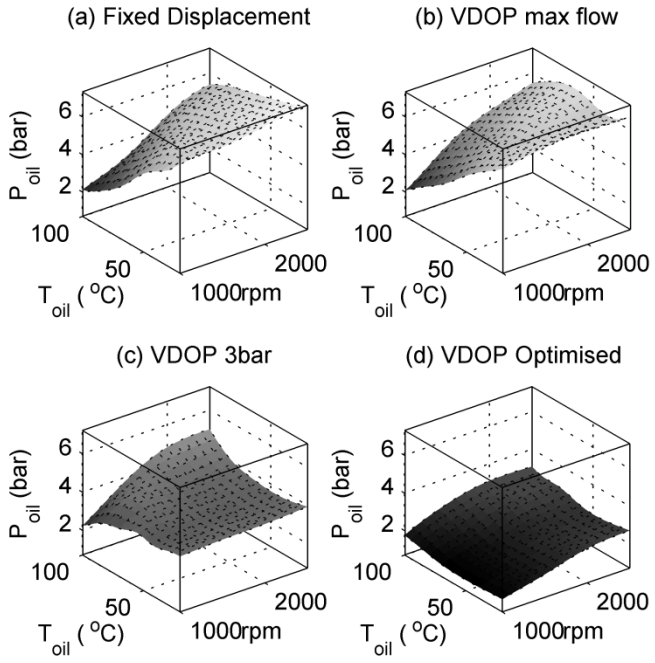

Figure 7: Pump delivery oil pressure against engine speed and oil temperature for (a) fixed displacement pump, (b) max flow VDOP, (c) flat map VDOP and (d) optimized VDOP

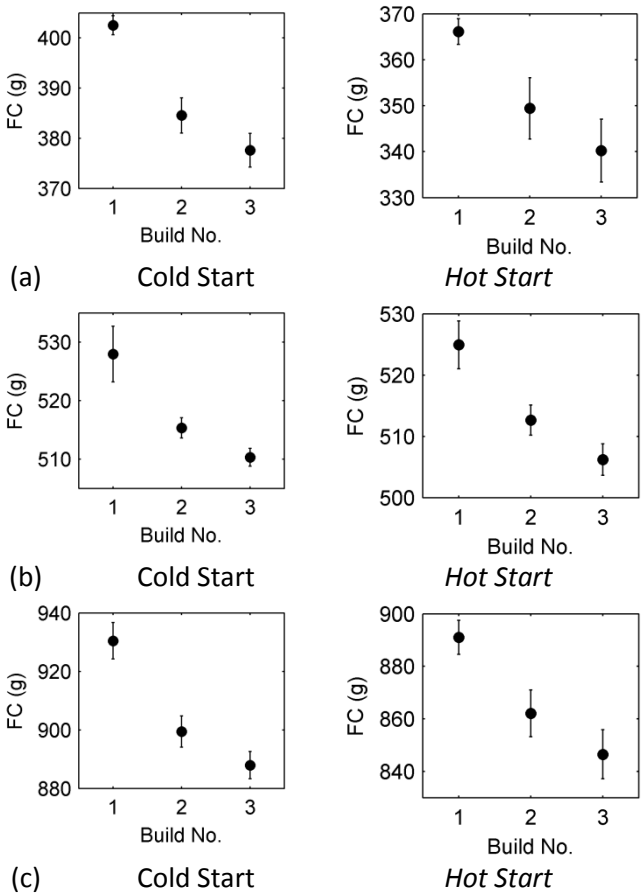

Figure 8: Cold and hot start fuel consumption for (a) ECE, (b) EUDC and (c) NEDC for three oil pump control settings

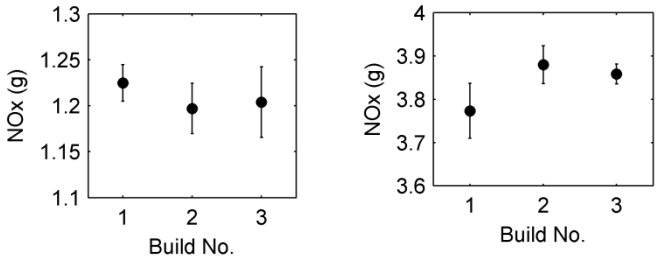

(a) ECE NO_x

(b) EUDC NO_x

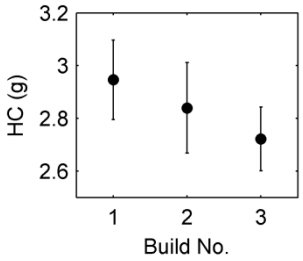

(c)ECE HC

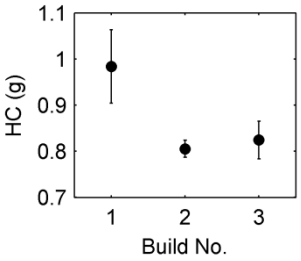

(d) EUDC HC

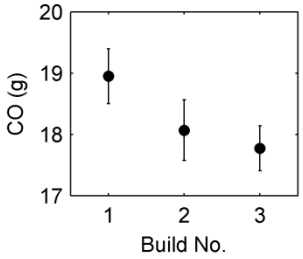

(e) ECE CO

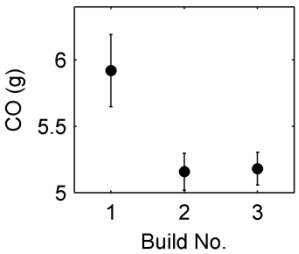

(f) EUDC CO

Figure 9: Cold-start (a), (b) NOx, (c), (d) HC and (e), (f) CO emissions over ECE and EUDC for three oil pump configurations

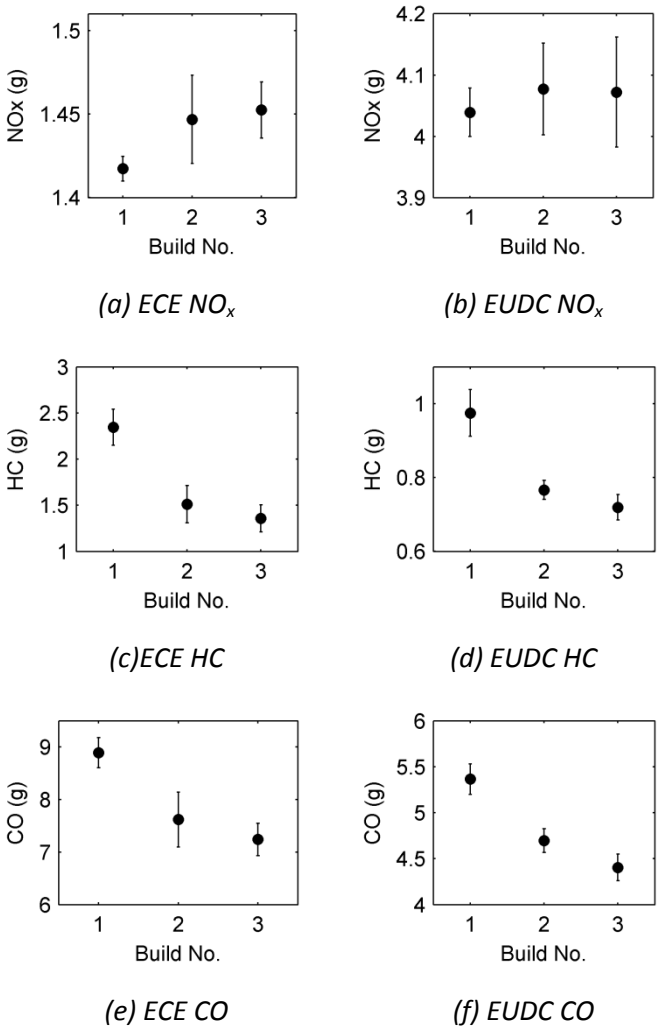

(a) ECE NO_x *(b) EUDC NO_x*

(c)ECE HC *(d) EUDC HC*

(e) ECE CO *(f) EUDC CO*

Figure 10: Hot-start (a), (b) NOx, (c), (d) HC and (e), (f) CO emissions over ECE and EUDC for three oil pump configurations

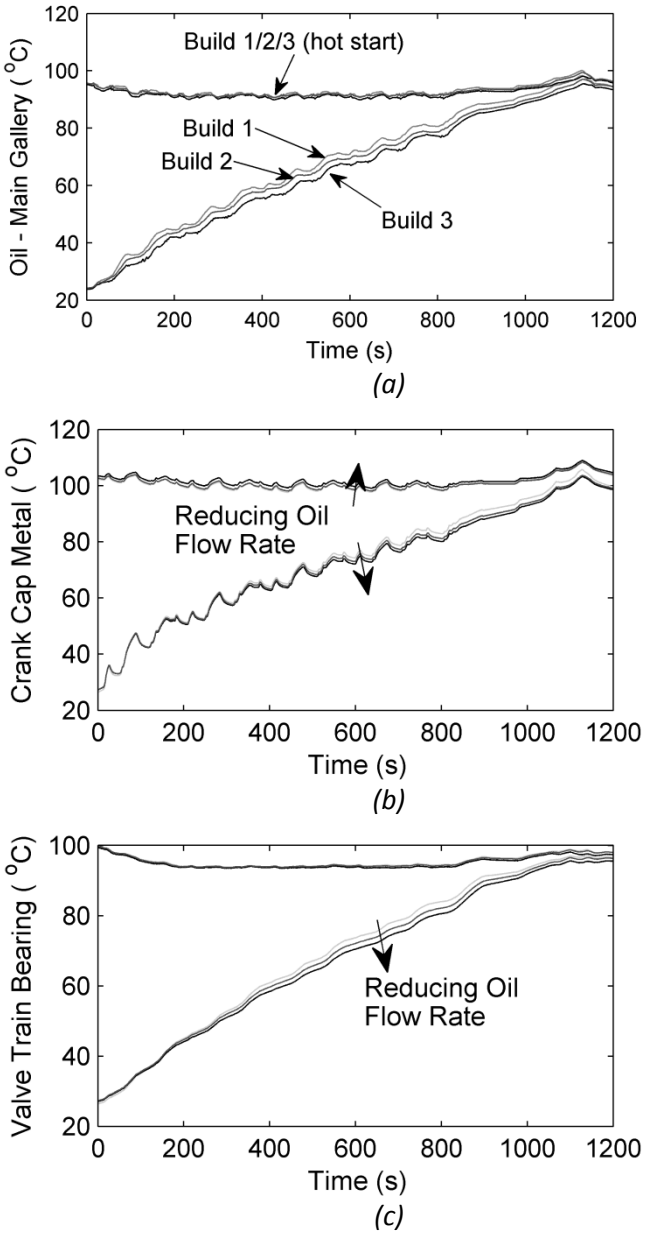

Figure 11: (a) Oil main gallery, (b) cranks shaft bearing cap and (c) Valve train bearing cap temperatures for hot and cold start NEDC and for builds 1, 2 and 3

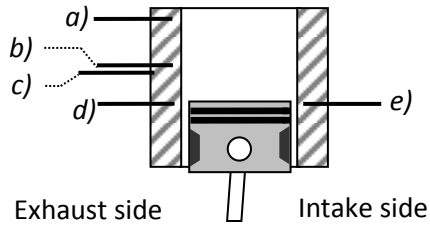
a)
b)
c)
d)
e)
Exhaust side
Intake side

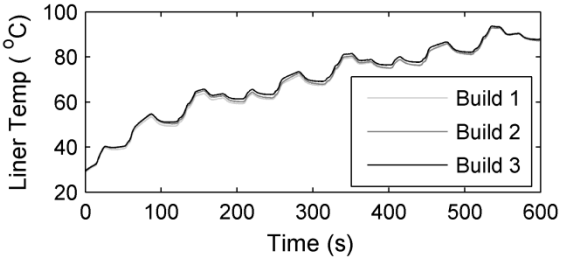
Liner Temp (°C)
Time (s)
Build 1
Build 2
Build 3

(a)

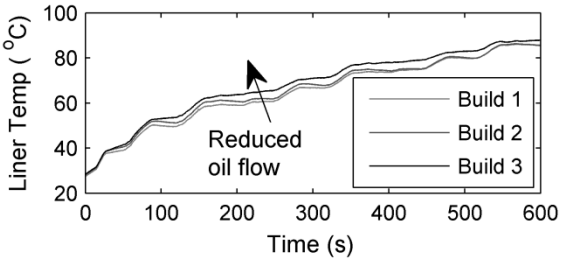
Liner Temp (°C)
Time (s)
Reduced
oil flow
Build 1
Build 2
Build 3

(b)

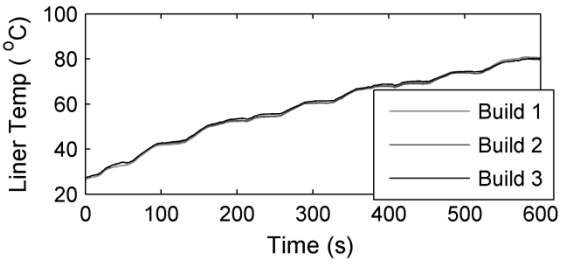
Liner Temp (°C)
Time (s)
Build 1
Build 2
Build 3

(c)

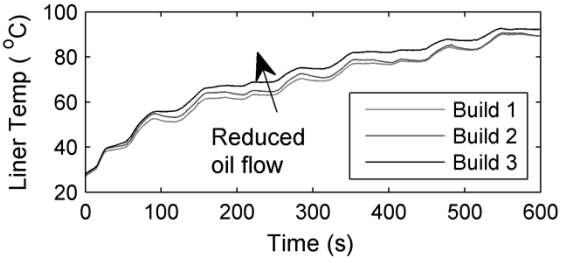
Liner Temp (°C)
Time (s)
Reduced
oil flow
Build 1
Build 2
Build 3

(d)

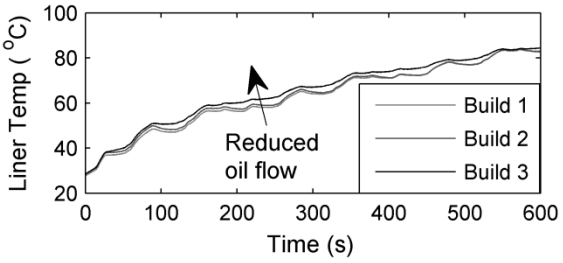

(e)

Figure 12: Selected liner temperatures over first 600s of cold-start NEDC for three oil pump configurations

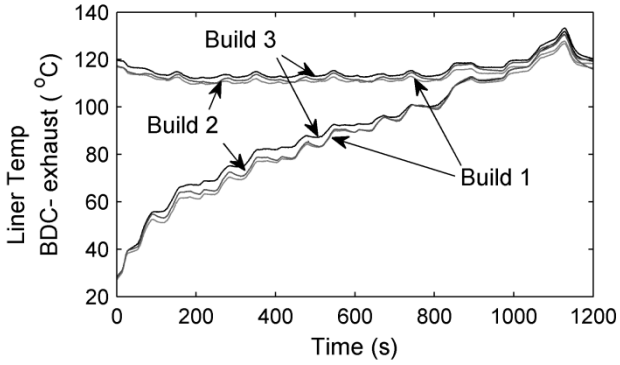

Figure 13: Cylinder liner temperature on exhaust side, 2mm from inner wall near bottom dead centre for cold- and hot-start NEDC AND for three oil pump configurations

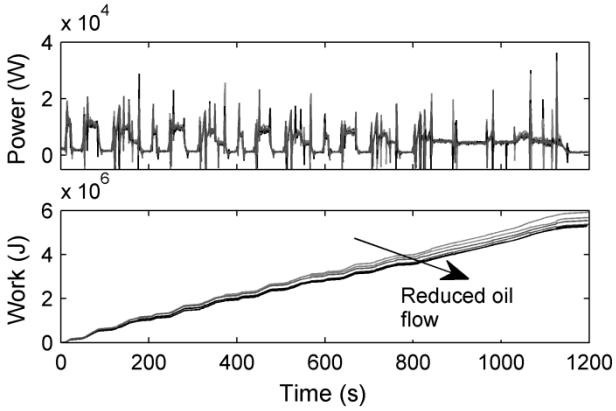

Figure 14: Friction and accessory power and work over NEDC for three VDOP calibrations showing reduced work with reduced oil flow

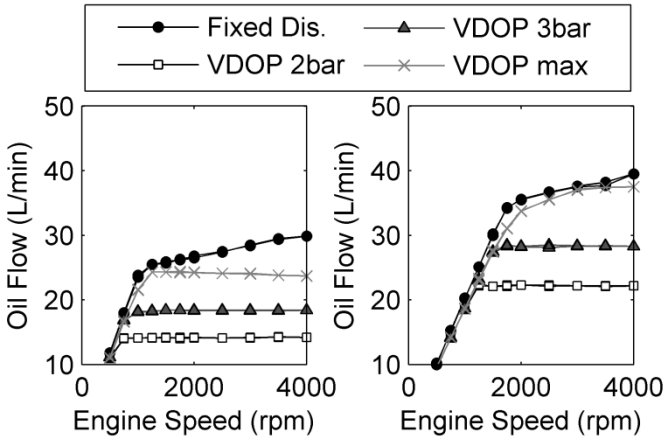

Figure 15: Oil flow rates measured on test stand at (a) 60°C and (b) 110°C oil temperature for fixed displacement oil pump and VDOP at varying target pressures

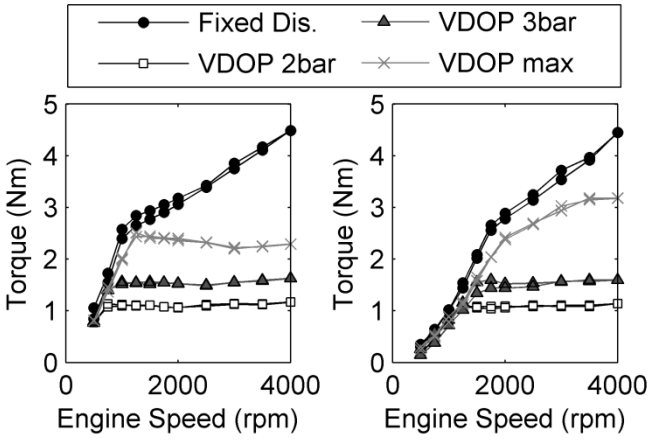

Figure 16: pump driving torque measured on test stand at (a) 60°C and (b) 110°C oil temperature for fixed displacement oil pump and VDOP at varying target pressures

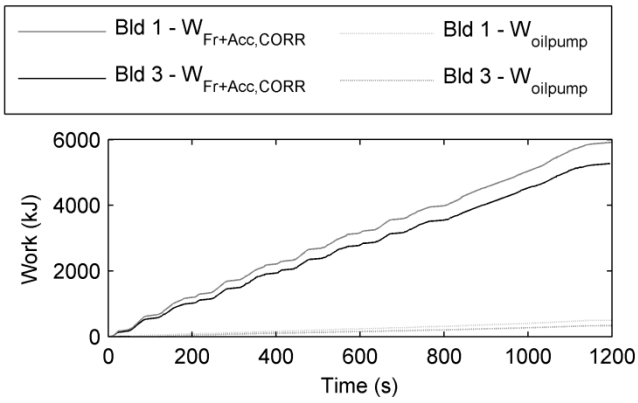

(a)

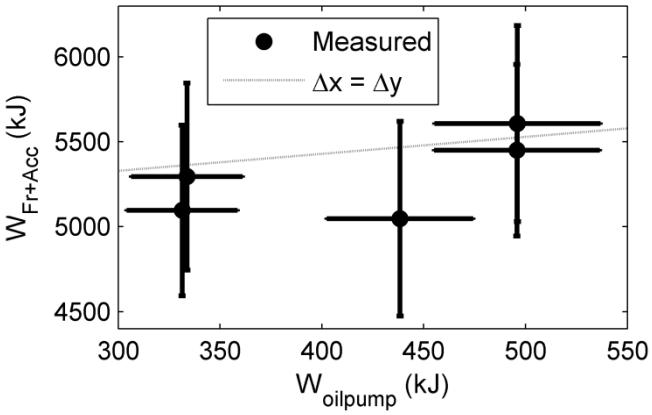

(b)

Figure 17: Total friction (friction + accessory load) and oil pump energy consumption, (a) detailed comparison of Build 1 and 3 over NEDC and (b) summary for all test points